Changes in Northern Hemisphere stratospheric variability under increased CO2 concentrations. Q J R Meteorol Soc

ARTICLE *in* QUARTERLY JOURNAL OF THE ROYAL METEOROLOGICAL SOCIETY · JULY 2010

Impact Factor: 3.25 · DOI: 10.1002/qj.633

3 AUTHORS, INCLUDING:

L. J. Gray
University of Oxford
147 PUBLICATIONS **4,377** CITATIONS

RMetS
Royal Meteorological Society

Changes in Northern Hemisphere stratospheric variability under increased CO_2 concentrations

Christopher J. Bell,[a]*Lesley J. Gray[a] and Jamie Kettleborough[b†]
[a] *Department of Meteorology, University of Reading, UK*
[b] *Hadley Centre, Met Office, Exeter, UK*
*Correspondence to: C. J. Bell, Department of Meteorology, University of Reading, Earley Gate, PO Box 243, Reading, RG6 6BB, UK. E-mail: c.bell@reading.ac.uk
† The contribution of J. Kettleborough was written in the course of his employment at the Met Office, UK, and is published with the permission of the Controller of HMSO and the Queen's Printer for Scotland.

The robustness of stratospheric circulation changes under increased concentrations of carbon dioxide are investigated using the Met Office HadSM3-L64 model. Equilibrium climate change simulations employing forcing of two and four times pre-industrial CO_2 are presented, with particular focus on the temperature response of the Arctic lower stratosphere during Northern Hemisphere winter. High CO_2 loading provides the ability to attain the statistical significance of any response, typically a problem given the large component of interannual variability common to the region. In response to CO_2, the expected global stratospheric cooling is modified by an anomalous dynamical warming of the Arctic winter lower stratosphere. This warming is shown to be associated with an increase in frequency of stratospheric sudden warming (SSW) events. At four times pre-industrial CO_2, the frequency of SSW events per year is doubled with respect to the control simulation. Further, by comparing winters with and without SSW events, it is shown that the warming of the lower stratosphere cannot be achieved without the presence of a frequency modulation of SSW events.

Key Words: climate change; stratospheric sudden warmings; Northern Annular Mode

Received 19 January 2010; Revised 29 March 2010; Accepted 11 April 2010; Published online in Wiley InterScience 8 July 2010

Citation: Bell CJ, Gray LJ, Kettleborough J. 2010. Changes in Northern Hemisphere stratospheric variability under increased CO_2 concentrations. *Q. J. R. Meteorol. Soc.* **136**: 1181–1190. DOI:10.1002/qj.633

1. Introduction

In the stratosphere, the well-established radiative response to enhanced concentrations of carbon dioxide is that of a global cooling, increasing in magnitude from the tropopause to the stratopause (Fels *et al.*, 1980). From observations of recent stratospheric temperature trends, this global stratospheric cooling has been well documented (Ramaswamy *et al.*, 2001; WMO, 2006). Randel *et al.* (2009) present a recently updated observational analysis of stratospheric temperature trends between 1979 and 2007 which show evidence of cooling trends reaching $\sim$0.5 K decade^{-1} and $\sim$1.5 K decade^{-1} in the lower and upper stratosphere, respectively. General circulation model (GCM) climate change studies robustly demonstrate this global stratospheric cooling, both in simulations of the recent past (Shine *et al.*, 2003; Eyring *et al.*, 2006) and in projections of future stratospheric temperature trends (Austin *et al.*, 2003; Eyring *et al.*, 2007).

In light of the robustness of *global* stratospheric cooling, the same cannot be said for *local* stratospheric temperature trends, in particular those in the Northern Hemisphere (NH) high latitudes during boreal winter. Satellite and radiosonde observations demonstrate no statistically significant cooling in the Arctic lower stratosphere (ALS) during December–February (DJF) over the past 25 years (Thompson and Solomon, 2005; Randel *et al.*, 2009), and GCM studies typically simulate ALS temperature trends that are statistically indistinguishable from zero

(Shine *et al.*, 2003). Projections of 21st century ALS temperature trends from GCM studies which incorporate interactive stratospheric chemistry also lack consistency, with statistically insignificant trends varying in both magnitude and sign between different models (e.g. Austin *et al.*, 2003; Eyring *et al.*, 2007). Somewhat more consistent are the ALS temperature responses reported in equilibrium climate change modelling studies, focusing on the stratospheric response to a fixed increase in CO_2 concentration. Several studies report a warming of the Arctic lower stratosphere, albeit not statistically different from zero, and a weakening of the wintertime stratospheric polar vortex (Rind *et al.*, 1998; Schnadt *et al.*, 2002; Gillett *et al.*, 2003; Sigmond *et al.*, 2004; Fomichev *et al.*, 2007).

Lack of a robust temperature response, however, is perhaps not surprising given that (1) any temperature trend in the wintertime ALS will likely be small in amplitude, due the close balance between enhanced diabatic CO_2 cooling and the predicted adiabatic warming accompanying a strengthened mean-meridional circulation (Butchart *et al.*, 2006; McLandress and Shepherd, 2009b) and (2) trends may also be contaminated by the large component of interannual variability common to the region, in particular that due to the occurrence of stratospheric sudden warming (SSW) events.

The predicted changes in stratospheric wave drag that influence the mean-meridional circulation (Butchart *et al.*, 2006; Garcia and randel, 2008; McLandress and Shepherd, 2009b) are also likely to have an impact on the variability of the NH polar vortex, although relatively few studies to date have explicitly investigated such a possibility. In a $2\times CO_2$ simulation, Rind *et al.* (1998) reported a decrease in the frequency of SSW events compared to their control simulation. More recently, in a comprehensive study using the Geophysical Fluid Dynamics Laboratory model, Charlton-Perez *et al.* (2008) report a small (but significant) increase in frequency of SSW events during the 21st century. McLandress and Shepherd (2009a) also report a frequency increase of SSW events in response to 21st century CO_2 concentrations, but suggest that the change is solely dependent on SSW definition, such that the absolute criterion of zonal-mean zonal wind reversal at 10 hPa and 60°N is more easily met given a weaker climatological polar vortex response in the mean state. The possibility of greenhouse-gas-related changes in stratospheric variability therefore requires further investigation. Evidence of a stratospheric influence on the tropospheric response to climate change (Scaife *et al.*, 2005; Huebener *et al.*, 2007; Dall'Amico *et al.*, 2010; Sigmond and Scinocca, 2010) also implies that modelled changes in stratospheric variability may be important in correctly determining the surface climate change projections.

In this paper we examine the robustness of the stratospheric response to changes in CO_2 concentrations, with particular focus on the variability of the NH winter polar vortex. Using a state-of-the-art stratosphere-resolving GCM under high CO_2 loading, experiments are performed which aim to increase the signal-to-noise ratio such that any signal associated with CO_2-induced changes to the NH polar vortex can be detected above the noise of background natural variability. A $4\times CO_2$ experiment has been carried out and results are compared to the $2\times CO_2$ experiment described in Gillett *et al.* (2003). The results show that, contrary to radiative considerations, a warming of the ALS is present during NH winter and appears robust under higher CO_2 loading. This warming is dynamical in origin and results indicate that it may only be accounted for in terms of a frequency modulation of SSW events.

2. Model and experimental design

The model used for the simulations described in this paper is the Met Office HadSM3-L64, as described by Gillett *et al.* (2002). This version is based on the third Hadley Centre Atmosphere Model (HadAM3, Pope *et al.*, 2000) and coupled to a 50 m mixed-layer ocean and sea-ice model. The slab ocean allows sea-surface temperatures (SSTs) to adjust to the changing radiative forcing and provides a more interactive lower-boundary condition with respect to integrations performed with prescribed SSTs.

The model has a horizontal atmospheric latitude–longitude resolution of $2.5^\circ \times 3.75^\circ$ and, of importance to this study, includes representation of a well-resolved stratosphere, with 64 vertical levels extending from the surface up to 0.01 hPa, 38 of which are above 100 hPa. The parametrization of subgrid-scale orographic gravity-wave drag is that of Gregory *et al.* (1998) and a Rayleigh friction is applied to model upper layers for stability purposes. The radiative transfer scheme is that developed by Edwards and Slingo (1996), and prescribed ozone fields used are taken from the zonal-mean monthly-mean climatology of Li and Shine (1995). To simulate pre-industrial ozone conditions, empirical corrections were applied (described in Gillett *et al.*, 2003) to increase ozone concentrations throughout the stratosphere and replenish the Antarctic ozone hole.

Three equilibrium climate change experiments have been carried out; a control run (CTRL), a doubled CO_2 run (2XCO2) and a quadrupled CO_2 run (4XCO2). The CTRL and 2XCO2 integrations are identical to those described by Gillett *et al.* (2003) and prescribe volume mixing ratios of 287 ppmv (representative of pre-industrial CO_2 concentrations) and 578 ppmv (predicted to occur around the year 2060 according to the IPCC AR4 A1B scenario) respectively. To increase the signal-to-noise ratio of any climate change response in the NH polar vortex, a third run (4XCO2) has been carried out with atmospheric CO_2 concentrations quadrupled to 1138 ppmv. Ozone values have been fixed at their pre-industrial concentrations for all three runs. The experiments have been carried out for 25, 35 and 30 years respectively, following spin-up to quasi-equilibrium.

The majority of results presented will be shown as responses i.e. differences between each experiment and the CTRL simulation. To represent statistical significance, responses will be plotted along with 95% confidence levels, where applicable, and significance is based on the Student's *t*-test (Wilks, 1995).

3. Results

3.1. Monthly mean response

The December–January averaged zonal-mean temperature response to changing CO_2 amounts is shown in Figure 1. For both 2XCO2 and 4XCO2 experiments, there is a clear tropospheric warming and stratospheric cooling, as expected from radiative considerations (Fels *et al.*, 1980). When CO_2 concentrations rise, the increased thermal emissivity of the stratosphere enhances its ability to radiate to space,

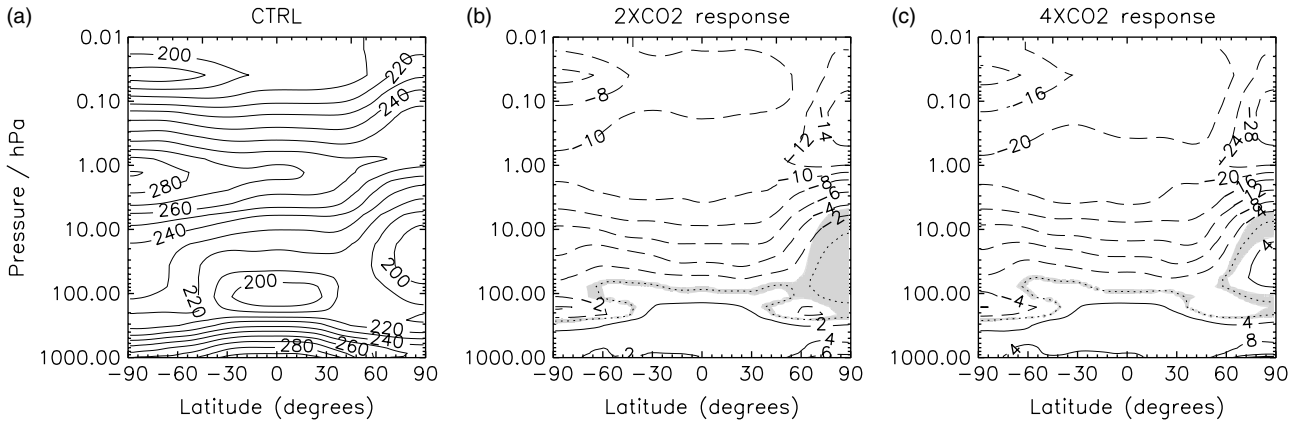

Figure 1. December–January mean zonally averaged temperature for (a) the CTRL, (b) the 2XCO2 response and (c) the 4XCO2 response. Contour intervals are (a) 10 K, (b) 2 K and (c) 4 K. Shading indicates regions where there is no significant response at the 95% level, according to a Student's *t*-test.

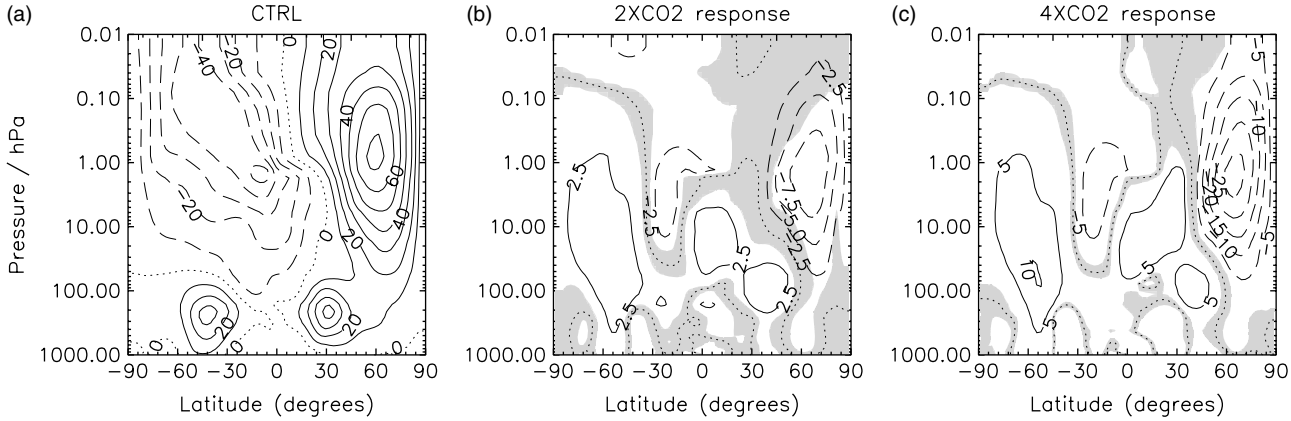

Figure 2. As Figure 1, but for December–January monthly mean zonally averaged zonal wind. Contour intervals are (a) 10 m s^{-1}, (b) 2.5 m s^{-1} and (c) 5 m s^{-1}.

providing a cooling trend. Although increased stratospheric CO_2 also implies an enhancement of thermal infrared absorbtivity, an increase in tropospheric opacity means that increased absorption of upwelling radiation is small with respect to increased emission, leading to the observed vertical structure of a cooling with height in the stratosphere (Fels *et al.*, 1980; Ramaswamy *et al.*, 2001).

The expected global-mean vertical structure of cooling can be seen throughout the stratosphere in Figure 1, increasing with height from the lower stratosphere and reaching a peak near the stratopause. For 2XCO2, the December–January global-mean stratopause cooling reaches ∼11 K, and cools locally by ∼14 K over the mesospheric NH polar-cap. An exception to the global stratospheric cooling is seen in the ALS region where, contrary to radiative considerations, there is a warming response. This dynamical temperature signal at doubled CO_2 reaches ∼1.5 K but is not statistically significant. In the 4XCO2 experiment, however, this warming response has increased to ∼4 K and is highly statistically significant. Contours for the 4XCO2 experiment are double those of the 2XCO2 experiment, giving an indication of the linearity of the response. Outside of the NH polar-cap region, the response to CO_2 does appear strongly linear, indicating radiative control of stratospheric temperatures. However, within the vortex region the temperature response is nonlinear, implying that the ALS warming is associated with a dynamical response of the polar vortex.

The corresponding zonal-mean zonal wind responses are shown in Figure 2. In the NH there is a substantial weakening of the polar vortex throughout the depth of the stratosphere. The statistically insignificant temperature response in the 2XCO2 experiment contrasts with the statistically significant zonal wind response above it, indicating that an integrated measure of temperature may be more beneficial and provide a more significant measure of temperature change in the region. In the quiescent Southern Hemisphere (SH) summer, the zonal-wind responses scale much more linearly between 2XCO2 and 4XCO2, suggesting the dominance of radiative and not dynamical control.

In the lower stratosphere the zonal-mean zonal wind changes near 40°N are consistent with the modelled temperature changes. Strong warming of the upper tropical troposphere relative to higher latitudes at the same altitude increases the meridional temperature gradient at the tropopause level and adjusts the zonal wind distribution in order to maintain the thermal wind relationship. This response is highly robust among climate change model simulations and appears as strengthened westerlies in the upper and poleward flank of the subtropical tropospheric jet (Lorenz and DeWeaver, 2007). In the troposphere, changes are manifest as an intensification of the winter storm-tracks (Yin, 2005). A significant strengthening of zonal winds can be traced, in both 2XCO2 and 4XCO2 experiments down to the surface near 40°N, appearing as a poleward shift in the midlatitude surface westerlies.

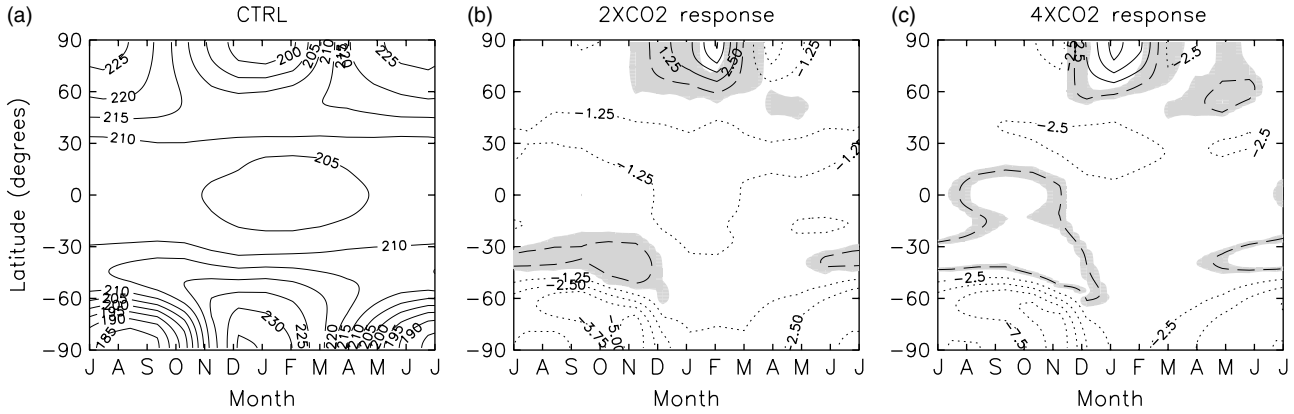

Figure 3. Contour plot of the zonal-mean temperature timeseries at 50 hPa, plotted against latitude for (a) CTRL, (b) 2XCO2 response and (c) 4XCO2 response. Contours are 5 K, 1.25 K and 2.5 K respectively. Shading denotes regions of no significant response at the 95% level.

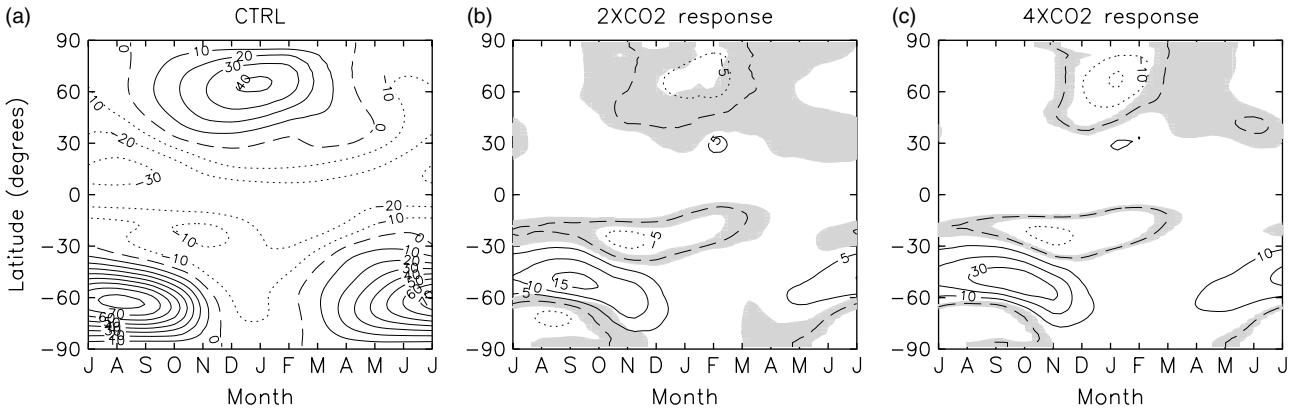

Figure 4. As Figure 3, but for zonal-mean zonal wind at 10 hPa. Contours are 10, 5 and 10 m s^{-1} respectively.

The time evolution of the monthly mean zonal-mean temperature response at 50 hPa is shown in Figure 3. In the 2XCO2 experiment, the warming reaches ∼3 K in February, and is significant only in this month over the NH pole. In the 4XCO2 experiment, the warming is significant throughout midwinter and maximises at ∼7.5 K in January. During late winter (February–April) there is no significant change in NH polar-cap temperatures on monthly time-scales. Higher Arctic temperatures during winter are accompanied by a weaker zonal-mean zonal winds at 10 hPa (Figure 4). In the 2XCO2 experiment, there is a weakening of the vortex by ∼5 m s^{-1} throughout the NH winter, peaking in February consistent with the warmest lower stratospheric temperature anomalies. The response appears robust at 4XCO2 with a significant zonal wind weakening of ∼20 m s^{-1}, maximising a month earlier than in the 2XCO2 experiment during December–January.

In contrast to the Arctic warming, the Antarctic stratosphere cools strongly throughout the SH winter in response to increased CO_2 concentrations. Cooling begins in the early southern winter, as the SH vortex is established, and maximises in November during SH spring. This spring cooling anomaly ultimately describes a delay in the final warming date of the vortex, which can be seen in the zonal wind responses near 60°S, which extend into December. At 2XCO2 the vortex cools in November by ∼5 K at 50 hPa, and by ∼10 K for the 4XCO2 vortex. The SH vortex is considerably strengthened on its equatorward side from May to December, maximizing during the vernal equinox. As opposed to the NH winter response, the cooling and strengthening of the SH vortex suggests that radiative influences dominate the modelled SH response, whereas dynamical influences are important in the NH winter.

3.2. *Daily response*

Changes in the variability of the NH polar vortex are now investigated on daily time-scales. Figure 5 shows the daily timeseries of absolute zonal-mean zonal wind at 10 hPa and 60°N. Each year is overplotted to give an indication of the interannual variability. The CTRL timeseries displays the common characteristics of flow in the extratropical NH stratosphere: easterlies dominate during the summer months, becoming westerly in September with the establishment of the wintertime polar vortex. As the vortex becomes more intense, large departures from the mean mark intermittent periods of wave-driven decelerated flow. Compared to the CTRL, the 2XCO2 simulation appears to demonstrate increased periods of variability during early winter. The weaker vortex shown in Figure 4 is evident in the daily climatology as a reduction in the amplitude of the seasonal cycle between December and March, although the reduction is only statistically significant during February. The 4XCO2 timeseries shows even greater variability throughout winter, especially during December–January when the climatological values are weakened by ∼50% of the CTRL and take on a double-peaked maximum over winter.

Measured more directly, the standard deviation, σ, of daily zonal-mean zonal wind at 10 hPa and 60°N provides

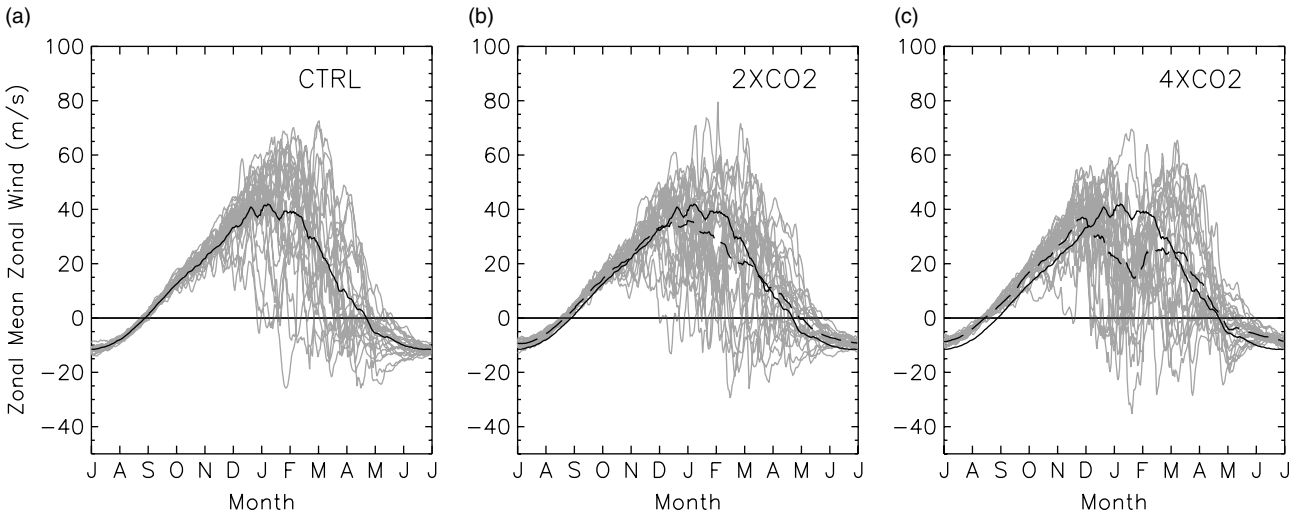

Figure 5. Daily timeseries of absolute zonal-mean zonal wind (m s^{-1}) at 10 hPa and 60°N for (a) CTRL, (b) 2XCO2 and (c) 4XCO2 simulations. 25 years of each experiment are overplotted in grey for comparison. The bold solid line on each denotes the daily climatology from the CTRL, and the dashed line that from the experiment.

a quantitative evaluation of interannual variability and is shown in Figure 6. The CTRL distribution maximises during winter months as expected, and is centred around February–March indicating that the model experiences most stratospheric variability in late winter –a common characteristic of stratosphere-resolving GCMs (Charlton *et al.*, 2007). Under increased CO_2 forcing, the vortex experiences a statistically significant increase in interannual variability. For the 2XCO2 experiment, significant increases in variability are apparent during November and December, indicating a more disturbed vortex earlier in the winter season. These changes, however, have no significant effect on the mean state temperatures of the vortex during early winter (Figure 3). The 4XCO2 experiment demonstrates a clear increase in early winter interannual variability. The increase is significant for prolonged periods throughout September–January. Anomalous variability of the 4XCO2 vortex peaks during December–January, and coincides with a significantly weaker and more disturbed climatological mean vortex (Figure 5).

The response of absolute ALS polar-cap temperatures can be examined using histograms, shown in Figure 7 as daily December–January North Pole temperatures at 50 hPa. The CTRL run exhibits a skewed distribution with a mean temperature centred at ∼197 K and a tail out to large positive values. This distribution describes the prevalence of a cold, strong winter vortex interspersed with infrequent SSW events. The 2XCO2 distribution exhibits a slightly higher mean temperature (1.5 K, consistent with Figure 1) and has a broader tail extending to higher temperatures, corresponding to a significant increase in standard deviation of 15%. A much flatter distribution is displayed for the 4XCO2 temperatures, dominated by an even broader tail than at 2XCO2. The mean is shifted by 5.5 K, and the increased standard deviation of 50% with respect to the CTRL distribution is highly significant. These CO_2 perturbed distributions suggest not only an influence of CO_2 on the mean state but also on the variability of the vortex. In particular, the broadened tails strongly imply a frequency modulation of SSW events.

3.3. *Identification of SSW events*

To measure changes in variability more directly, SSW events have been identified using the WMO (World Meteorological Organization) definition based on zonal-mean zonal wind. This method has been employed widely and forms the basis of the standard identification technique set out by Charlton and Polvani (2007). Here a major SSW is defined to occur when the daily zonal-mean zonal wind becomes easterly at 60°N and 10 hPa during the extended winter period (December–April). Dates on which the zonal-mean zonal wind reverses are defined as the central dates of the SSWs. Any other date within 30 d of an identified central date is discounted from the search for further events, so as not to double-count a SSW once it has started its lifecycle. This period is typically chosen as approximately twice the radiative time-scale of the mid-stratosphere (e.g. Shine, 1987).

Figure 8 shows the monthly distribution of major SSW frequency as events y^{-1}. The NCEP–NCAR data (National Centers for Environmental Prediction –National Center for Atmospheric Research) are shown in each, for comparison. The CTRL simulation not only exhibits a good climatology of SSWs (0.56 events y^{-1}), consistent with the observed SSW frequency of 0.6 events y^{-1} (Charlton and Polvani, 2007), but also provides an agreeable seasonal distribution of events. There is, however, a slight bias of SSW frequency to late winter, similarly expressed in the CTRL σ-distribution of Figure 6.

The 2XCO2 vortex exhibits an increased frequency of SSWs during NH winter of 0.71 events y^{-1} in total. The largest changes occur in December, consistent with the significant increase in early winter zonal-mean zonal wind σ, and no changes in frequency are noted in March. This temporal distribution indicates that more SSWs are forced in response to CO_2 during early winter but the timing of the final warming is not significantly affected. Robustness of this result is confirmed by the 4XCO2 simulation, which shows an approximate doubling (with respect to the CTRL) of SSW wintertime frequency from 0.56 to 1.20 events y^{-1}. As in the 2XCO2 experiment, changes in the monthly distribution of events are largely restricted to early winter, although

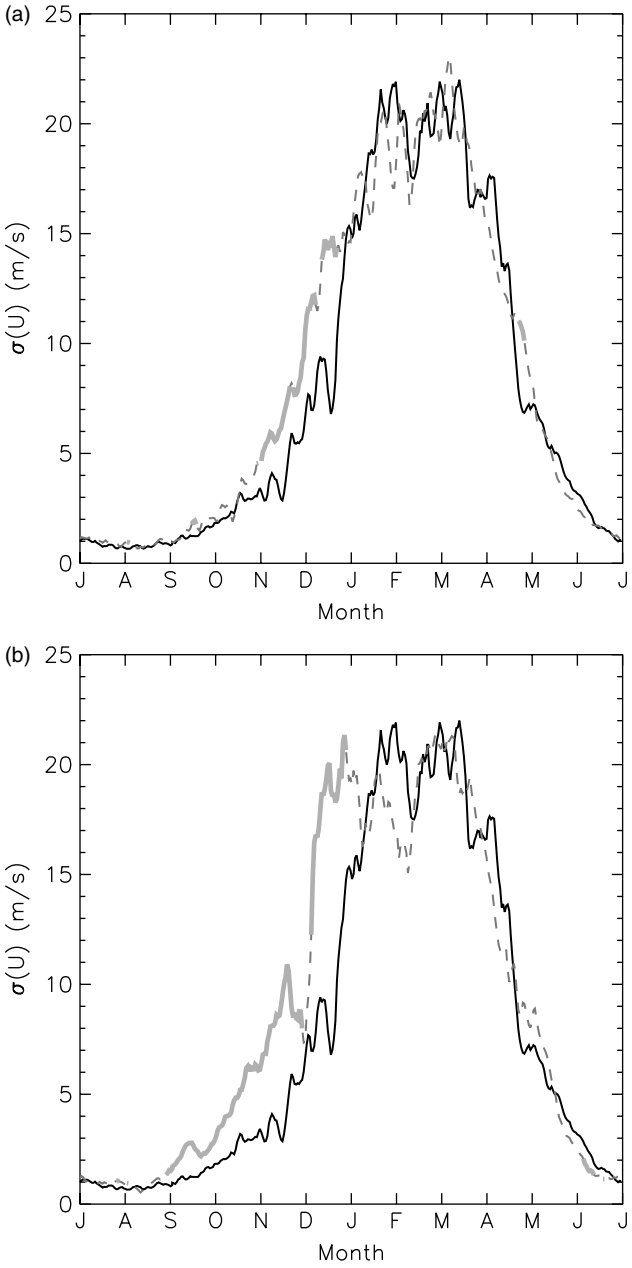

Figure 6. Daily standard deviation of zonal-mean zonal wind at 10 hPa and 60°N for the CTRL run (black line). The grey dashed line denotes that of the (a) 2XCO2 and (b) 4XCO2 simulations, overlain with a solid grey line where the standard deviations are different from the CTRL at the 95% level according to an f-test. Units are m s^{-1}.

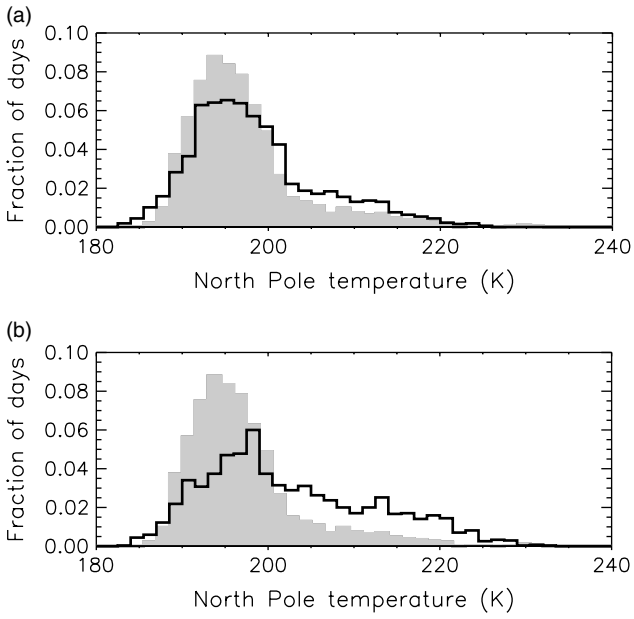

Figure 7. Normalised histograms of North Pole temperature (K) at 50 hPa during December–January for (a) 2XCO2 and (b) 4XCO2 simulations. Shaded grey histograms denote the CTRL and unfilled black lines each experiment.

the increase with respect to CO_2 appears highly nonlinear. In December, the 4XCO2 vortex undergoes 0.3 events y^{-1} compared to just 0.1 events y^{-1} in the CTRL run. The largest change is seen in January which undergoes 0.45 events y^{-1} compared to 0.2 events y^{-1} in the CTRL. Again the SSW frequency modulation reflects changes in the σ-distribution and temperature histograms shown previously.

Examination of the 4XCO2 zonal-mean zonal wind timeseries at 10 hPa and 60°N shows that in many years the vortex undergoes two SSWs through the winter. This can be seen in the double-peaked daily zonal wind climatology shown in Figure 5. Such a large increase in SSW frequency during December–January indicates that the vortex is, on average, being broken down earlier than usual in winter and has time to recover and undergo further dynamical breakdown in mid-late winter. This may explain the nonlinearity of the SSW response e.g. SSWs rely on a threshold vortex strength, which is easier to reach if the vortex has already been weakened by an earlier event. Also, there is only a finite period of time during the winter season, so there is an additional threshold in terms of timing of the first SSW and whether there is sufficient time remaining for a second SSW to be forced before the end of winter.

3.4. *Changes in SSW characteristics*

Given the large frequency modulation of SSW events, it is possible that the dynamics of SSWs may change in future climates. Several metrics have been derived (Table I) to quantify possible changes in their dynamical characteristics, and are similar to those proposed in Charlton and Polvani (2007). Note that, for each experiment, daily anomalies are taken as the departure of each field from the daily climatology of that particular experiment.

The first property is the area-weighted polar-cap (90–60°N) temperature anomaly at 10 hPa averaged ±5 d about the SSW central date. This metric gives an indication of the SSW magnitude and is denoted $\Delta\overline{T}_{10}$. The table shows that 10 hPa SSW magnitudes at 2 and 4 times CO_2 are not statistically different from those simulated in the CTRL experiment. There appears to be a linear decrease in temperature magnitude at 10 hPa: a 12% decrease for 2XCO2 and 24% decrease at 4XCO2. McLandress and Shepherd (2009a) also report a decrease in SSW temperature amplitude, however in these simulations the changes are not statistically significant. Therefore we cannot conclude that SSW amplitudes will be affected by changing CO_2 concentrations.

The second set of temperature metrics is similar to $\Delta\overline{T}_{10}$ but taken at 50 hPa and 100 hPa, averaged over 0–10 d after the central date. Denoted $\Delta\overline{T}_{50}$ and $\Delta\overline{T}_{100}$ respectively, these metrics provide a measure of the SSW influence on the

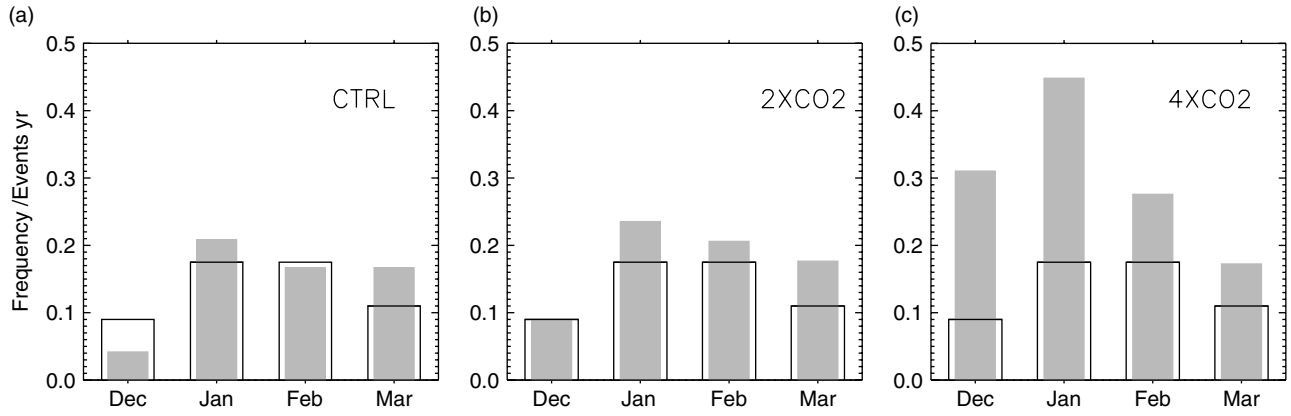

Figure 8. Bar charts of climatological monthly frequency of SSW events shown in grey for (a) CTRL, (b) 2XCO2 and (c) 4XCO2. Unfilled black bars show the observed SSW monthly climatology taken from NCEP–NCAR reanalysis.

Table I. Dynamical properties of SSW events as described in the text. Numbers in brackets denote the significance level of the difference between experiment and CTRL. Values below 0.05 denote significantly different means at the 95% level according to a Student's *t*-test.

	CTRL	2XCO2	4XCO2
Freq	0.56	0.71	1.20
$\Delta\overline{T}_{10}$ (K)	11.22	9.89 (0.59)	8.60 (0.25)
$\Delta\overline{T}_{50}$ (K)	6.98	6.85 (0.93)	5.63 (0.31)
$\Delta\overline{T}_{100}$ (K)	4.72	4.33 (0.64)	4.05 (0.38)
$\Delta\overline{U}_{10}$ ($m\,s^{-1}$)	24.17	27.89 (0.48)	23.20 (0.85)
*W*1:*W*2	2:1	2.5:1	4:1

Freq is frequency of SSW events y^{-1}.
*W*1:*W*2 is the ratio of wave-1 to wave-2 SSW events.

lower stratosphere and therefore the strength of downward anomaly propagation following a SSW event. At 50 hPa, amplitudes are decreased in comparison to the CTRL for both the 2XCO2 and 4XCO2 but not significantly so. At 100 hPa there appears to be a linear decrease in temperature anomalies with CO_2 concentration, but changes are again not statistically different from the CTRL.

Thirdly, the response of zonal-mean zonal wind gives a measure of the momentum deposition that accompanies a SSW i.e. it quantifies how strongly the vortex is decelerated. This is denoted $\Delta\overline{U}_{10}$ and taken as the change in zonal wind anomaly at 60°N and 10 hPa averaged between 15 and 5 d prior to the SSW and between 0 and 5 d after the central date. At 2XCO2 and 4XCO2 no significant differences are found from the CTRL experiment. All of these diagnostics therefore suggest that, while the frequency of SSWs increases under increased CO_2 concentrations, these essential characteristics remain unchanged and the influence on the Arctic lower stratospheric remains the same.

One characteristic that does appear to change with increased CO_2 concentration is the dominance of wave-1 (displacement) events over wave-2 (split) events. The CTRL experiment simulates a ratio of 2/1, which slightly increases in the 2XCO2 experiment to 2.5/1. However in the 4XCO2 experiment, virtually no vortex splitting events are simulated and displacement events totally dominate. This may be related to a significant increase in stationary wave-1 at 100 hPa (not shown), but requires further investigation.

3.5. *Influence of SSW frequency modulation on the mean climate*

Recent work has shown that the time-integrated composite polar-cap temperature response during a SSW, at 10 hPa, is approximately zero. This can be seen as a near-symmetric function centred around the composite SSW central date (Figure 4a of Charlton and Polvani, 2007). Negative temperature anomalies before and after the SSW event approximately balance the total time-integrated response to zero, suggesting little net influence on the mean-state temperature field. However, the same cannot be said for composite SSW temperature anomalies in the lower stratosphere at 100 hPa (Figure 4b of Charlton and Polvani, 2007a). Up to ∼60 d following a SSW, positive temperature anomalies dominate the distribution and are not balanced by a cooling, implying that the net effect on the mean winter state is non-zero in the lower stratosphere. Given that the inherent SSW characteristics appear unchanged in response to increased CO_2 concentrations, it is interesting to investigate the importance of SSW frequency modulation on the mean-state climate. Warming of the Arctic lower stratosphere during winter, with enhanced mesospheric cooling above (Figure 1), is almost certainly a signal of dynamical warming and may be a direct consequence of an increased frequency of SSW events.

One way to isolate the influence of major SSWs on the mean state of the lower stratosphere is to subdivide the time series into winters with and without a major SSW. This allows the mean winter response to CO_2 to be separated into those in which the stratosphere is either (1) strongly dynamically

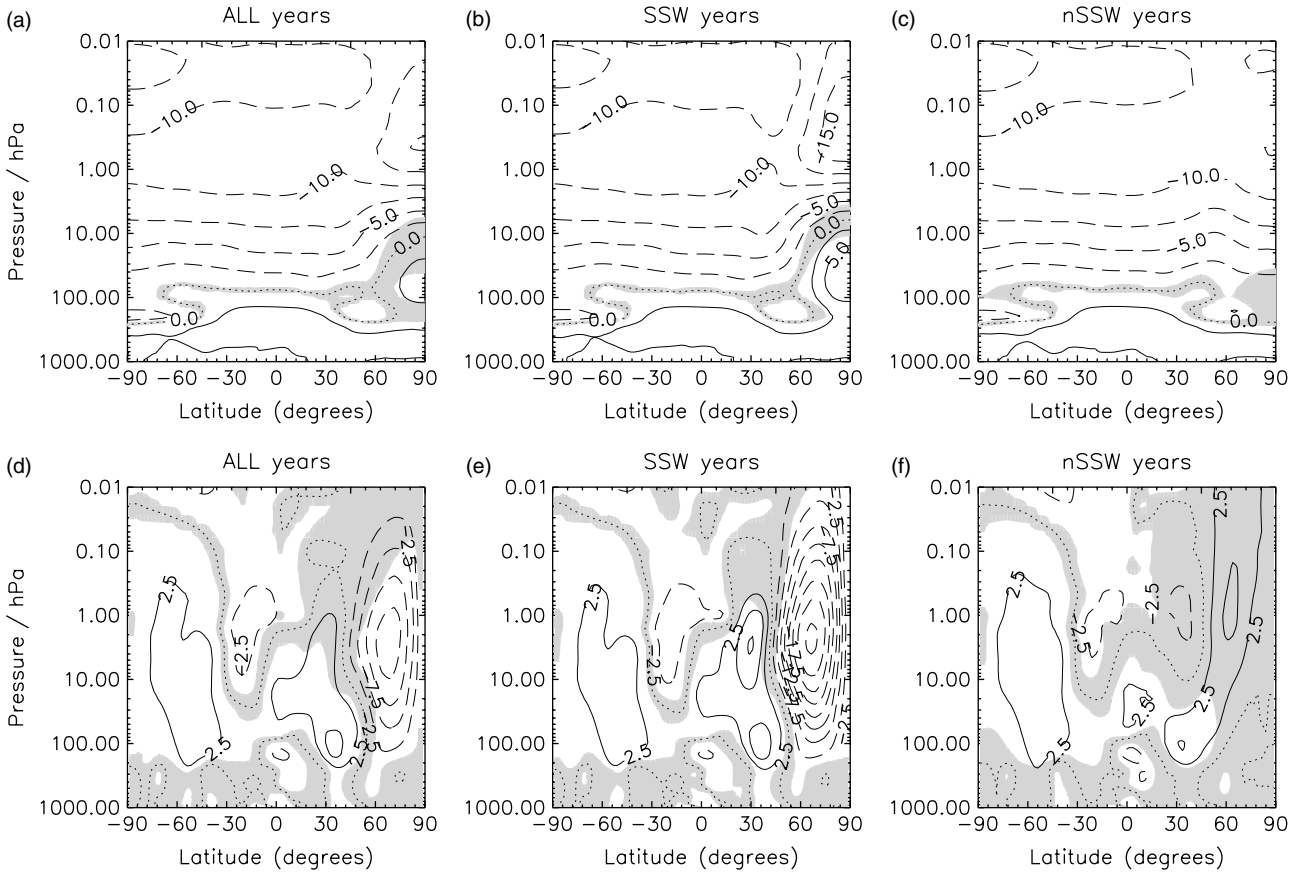

Figure 9. Mean January–February 2XCO2 response for zonal-mean (a, b, c) temperature (K) and (d, e, f) zonal wind ($m\,s^{-1}$). The response is subdivided into (a, d) all winters, (b, e) SSW winters and (c, f) non-SSW winters. Regions of no statistical significance at the 95% level are denoted by grey shading.

active, which by construction will include both radiative and dynamical responses to increased CO_2 concentrations or (2) dynamically quiet, whereby the stratospheric vortex is not broken down and temperature responses are dominated by radiative influences. Here, SSW winters are defined as one in which an SSW is identified during January–February. All other years are therefore defined as winters without, denoted nSSW. Note that this diagnostic is only suitable for the 2XCO2 experiment, as almost every winter season in the 4XCO2 simulation included an SSW event. For this reason a January–February winter period was chosen, as these are the only months during which the lower stratospheric warming is captured in the 2XCO2 experiments. Anomalies are taken from the CTRL monthly mean climatology.

Latitude–height composites of the zonal-mean temperature and zonal wind responses for January–February, and their decomposition into SSW and nSSW winters, are shown in Figure 9. The full 2XCO2 temperature response shows the typical stratospheric global cooling and a significant warming of the Arctic lower stratosphere reaching 2.5 K. This warming is dominated by the February response, which can be seen from the timeseries in Figure 4. The average temperature response during winters with an SSW includes a strong warming of the lower stratosphere of up to 5 K. Outside the NH polar-cap region, the temperature response is virtually identical to the full mean-state response. During nSSW winters, the Arctic lower stratosphere warming is not captured and the region cools. A closer symmetry with the dynamically inactive SH summer hemisphere is visible, where a similar cooling of ∼1–2 K is likely associated with a purely radiative response. Nevertheless, the NH does not cool as much as the SH, e.g. near 100 hPa. Although the retained winters do not include major SSWs, they still exhibit minor warmings and are more disturbed than the SH, which explains the region of statistical insignificance in the NH lower stratosphere.

The zonal wind responses show similar features (Figure 9(d, e, f)). The full 2XCO2 response appears as a weakened vortex throughout the NH winter stratosphere. Winters with SSW events reflect this 2XCO2 mean-state response, albeit with stronger anomalies. Significant intrusions into the troposphere are captured only during SSW winters. The same cannot be said for nSSW winters in which there is no significant change throughout the NH stratosphere or troposphere.

To better quantify the influence of SSW frequency modulation on the warming of the Arctic lower stratosphere, Figure 10 shows histograms of the daily January–February temperature anomalies. The CTRL histogram (Figure 10(a)) shows typical features; a positively skewed distribution with a tail out to positive values. The black line demonstrates that the tail is composed almost entirely from SSW winter days while the bulk of the distribution is composed from the much more frequent cold, strong vortex, winter days (dashed line). At 2XCO2 (Figure 10(b)), the mean distribution is much flatter with a significantly broader tail than the CTRL. The mean has shifted to ∼2.5 K and there is a substantial increase in the frequency of warm vortex days, i.e. days in the 5–20 K anomaly band. This increase is entirely composed of days during SSW winters. In fact, of the 940 winter days with a temperature anomaly greater than 2.5 K, 820 (87%) of those days are during SSW winters. If the 2XCO2 warming

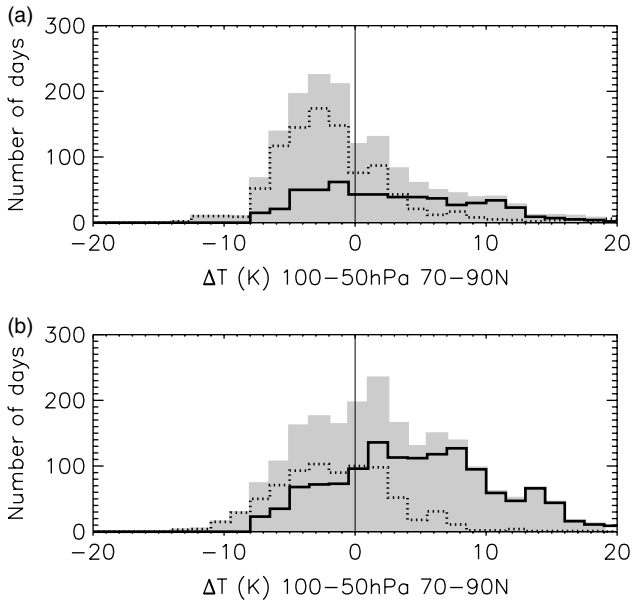

Figure 10. Histograms of the area-weighted daily January–February temperature anomaly (K) for 100–50 hPa and 70–90°N. Filled grey histograms contain all daily data from (a) CTRL and (b) 2XCO2 experiments. Dashed histograms contain only daily data from nSSW winters, and solid black lines contain daily data from SSW winters.

was simply due to a mean-state change then the nSSW days (dashed line) would also contribute to the broadened tail. This is not the case. The result strongly implies that the frequency modulation of SSW events influences temperatures in the Arctic lower stratosphere.

4. Summary and discussion

The influence of increased concentrations of CO_2 on the mean state and variability of the stratospheric polar vortex has been investigated using the Hadley Centre HadSM3-L64 model. Due to the large component of natural variability common to the Arctic lower stratosphere during NH winter, this study has concentrated on model simulations under a very high CO_2 loading. Concentrations of four times pre-industrial CO_2 have been used in order to establish statistical significance as, under doubled CO_2 concentrations, it appears unlikely that any signal associated with dynamical changes to the NH polar vortex will be detectable against the noise of background natural variability (e.g. Gillett *et al.*, 2003; Sigmond *et al.*, 2004).

With doubled CO_2 concentrations, contrary to radiative considerations, the Arctic lower stratosphere (ALS) undergoes a dynamical warming of up to 2.5 K between ∼100 and 10 hPa during the NH winter. This statistically insignificant response more than doubles and becomes highly significant at $4\times CO_2$ describing a robust weakening and warming of the polar vortex. Whilst most modelling studies within the stratospheric climate-change framework focus on the future mean state, this study concentrates on future changes in stratospheric variability, in particular that associated with the NH winter polar vortex. Both 2XCO2 and 4XCO2 experiments exhibit a statistically significant increase in early winter variability, as measured by the standard deviation of zonal wind at 10 hPa and 60°N. Histograms of the daily North Pole temperature at 50 hPa display much flatter distributions with increasing CO_2 whereby broadened positive tails indicate an increased frequency of anomalously warm vortex events. Measuring SSW events directly, using the WMO definition, a doubling in frequency from 0.56 to 1.20 events y^{-1} is found between the CTRL and 4XCO2 simulations. No significant changes in SSW characteristics are found, confirming the robustness of not only the 2XCO2 response but also the results of Charlton-Perez *et al.* (2008) and more recently McLandress and Shepherd (2009a).

The final part of this work concerns the influence of a frequency modulation of SSW events on the mean state. Previous studies attribute the winter ALS temperature anomaly to a strengthened mean meridional circulation (Sigmond *et al.*, 2004), such that stronger seasonal-mean extratropical downwelling will act to adiabatically warm the lower stratosphere and overcome the diabatic cooling due to enhanced CO_2 levels. However, few studies have examined the potential influence of changes in polar vortex variability on the mean state. McLandress and Shepherd (2009a) argue against this possibility by demonstrating that, in future climates, SSW frequency does not change when using a definition based on the Northern Annular Mode (NAM) (Baldwin and Thompson, 2009). The NAM-based definition neatly avoids using an SSW criterion dependent on the climatological mean state and is therefore a relative measure of variability about some control or perturbed mean state. They argue that, in the case of an increased CO_2 environment, use of the WMO absolute zonal-mean zonal wind criterion would erroneously identify an increased frequency of SSW events simply because the transition of zonal wind from westerly to easterly at 10 hPa and 60°N is more easily achieved given the weaker background zonal wind mean state. However, this NAM-based approach is critically dependent on the climatology from which anomalies are taken. In a transient climate-change simulation, this is difficult to define as one could assume that the climatological mean state is slowly evolving as the stratosphere compresses due to enhanced long-wave cooling. Importantly, the NAM approach also implicitly assumes that any change in SSW frequency does not contribute to a future climatological mean state. We concur that although true of the mid-stratosphere, the time-integrated winter temperature response to an SSW event is non-zero in the ALS (Charlton and Polvani, 2007), and thus SSW frequency modulation does have the potential to influence the winter-mean stratospheric state. We have demonstrated this by separating doubled CO_2 winters into those with and without SSW events, and show that the weakened vortex response can be attributed only to those winters during which a SSW occurs. Thus it is an SSW frequency modulation which contributes significantly to the mean-state warming of the ALS during NH winter. We suggest that the absolute SSW criterion is the appropriate parameter to assess future SSW frequency modulation as it is the absolute zonal winds which determine the propagation or otherwise of tropospheric planetary waves into the stratosphere.

Acknowledgements

This work was supported by a NERC studentship (NER/S/A/2005/13378), as well as CASE sponsorship from the UK Met Office. The authors would like to thank Nathan Gillett for providing the 2XCO2 simulations and also to

thank Elisa Manzini, Mike Blackburn and Andrew Charlton-Perez for useful discussions.

References

Austin J. Shindell D, Beagley SR, Brühl C, Dameris M, Manzini E, Nagashima T, Newman P, Pawson S, Pitari G, Rozanov E, Schnadt C, Shepherd TG. 2003. Uncertainties and assessments of chemistry-climate models of the stratosphere. *Atmos. Chem. Phys.* **3**: 1–27.

Baldwin MP, Thompson DWJ. 2009. A critical comparison of stratosphere-troposphere coupling indices. *Q. J. R. Meteorol. Soc.* **135**: 1661–1672.

Butchart N, Scaife AA, Bourqui M, de Grandpré J, Hare SHE, Kettleborough J, Langematz U, Manzini E, Sassi F, Shibata K, Shindell D, Sigmond M. 2006. Simulations of anthropogenic change in the strength of the Brewer Dobson circulation. *Clim. Dyn.* **27**: 727–741.

Charlton AJ, Polvani LM. 2007. A new look at stratospheric sudden warmings. Part I. Climatology and modelling benchmarks. *J. Climate* **20**: 449–469.

Charlton AJ, Polvani LM, Perlwitz J, Sassi F, Manzini E, Pawson S, Nielsen JE, Shibata K, Rind D. 2007. A new look at stratospheric sudden warmings. Part II. Evaluation of numerical model simulations. *J. Climate* **20**: 470–488.

Charlton-Perez AJ, Polvani LM, Austin J, Li F. 2008. The frequency and dynamics of stratospheric sudden warmings in the 21st century. *J. Geophys. Res. (Atmos.)* **113**: 16116, DOI: 10.1029/2007JD009571.

Dall'Amico M, Stott PA, Scaife AA, Gray LJ, Rosenlof KH, Karpechko AY. 2010. Impact of stratospheric variability on tropospheric climate change. *Clim. Dyn.* **34**: DOI: 10.1007/s00382-009-0580-1.

Eyring V, Butchart N, Waugh DW, Akiyoshi H, Austin J, Bekki S, Bodeker GE, Boville BA, Brühl C, Chipperfield MP, Cordero E, Dameris M, Deushi M, Fioletov VE, Frith SM, Garcia RR, Gettelman A, Giorgetta MA, Grewe V, Jourdain L, Kinnison DE, Mancini E, Manzini E, Marchand M, Marsh DR, d Nagashima T, Newman PA, Nielsen JE, Pawson S, Pitari G, Plummer DA, Rozanov E, Schraner M, Shepherd TG, Shibata K, Stolarski RS, Struthers H, Tian W, Yoshiki M. 2006. Assessment of temperature, trace species, and ozone in chemistry-climate model simulations of the recent past. *J. Geophys. Res. (Atmos.)* **111**: 22308, DOI: 10.1029/2006JD007327.

Eyring V, Waugh DW, Bodeker GE, Cordero E, Akiyoshi H, Austin J, Beagley SR, Boville BA, Braesicke P, Brühl C, Butchart N, Chipperfield MP, Dameris M, Deckert R, Deushi M, Frith SM, Garcia RR, Gettelman A, Giorgetta MA, Kinnison DE, Mancini E, Manzini E, Marsh DR, Matthes S, Nagashima T, Newman PA, Nielsen JE, Pawson S, Pitari G, Plummer DA, Rozanov E, Schraner M, Scinocca JF, Semeniuk K, Shepherd TG, Shibata K, Steil B, Stolarski RS, Tian W, Yoshiki M. 2007. Multimodel projections of stratospheric ozone in the 21st century. *J. Geophys. Res. (Atmos.)* **112**: 16303, DOI: 10.1029/2006JD008332.

Fels SB, Mahlman JD, Schwarzkopf MD, Sinclair RW. 1980. Stratospheric sensitivity to perturbations in ozone and carbon dioxide: Radiative and dynamical response. *J. Atmos. Sci.* **37**: 2265–2297.

Fomichev VI, Jonsson AI, de Grandpré J, Beagley SR, McLandress C, Semeniuk K, Shepherd TG. 2007. Response of the middle atmosphere to CO2 doubling: Results from the Canadian Middle Atmosphere Model. *J. Climate* **20**: 1121.

Garcia RR, Randel WJ. 2008. Acceleration of the Brewer–Dobson circulation due to increases in greenhouse gases. *J. Atmos. Sci.* **65**: 2731–2739.

Gillett NP, Allen MR, Williams KD. 2003. Modelling the atmospheric response to doubled CO2 and depleted stratospheric ozone using a stratosphere-resolving coupled GCM. *Q. J. R. Meteorol. Soc.* **129**: 947–966.

Gillett NP, Allen MR, Williams KD. 2002. The role of stratospheric resolution in simulating the Arctic Oscillation response to greenhouse gases. *Geophys. Res. Lett.* **29**: 10.

Gregory D, Shutts GJ, Mitchell JR. 1998. A new gravity-wave-drag scheme incorporating anisotropic orography and low-level wave breaking: Impact upon the climate of the UK Meteorological Office Unified Model. *Q. J. R. Meteorol. Soc.* **124**: 463–493.

Huebener H, Cubasch U, Langematz U, Spangehl T, Niehörster F, Fast I, Kunze M. 2007. Ensemble climate simulations using a fully coupled ocean-troposphere-stratosphere general circulation model. *Phil. Trans. R. Soc. London A: Math. Phys. Eng. Sci.* **365**: 2089–2101.

Li D, Shine KP. 1995. *A four-dimensional ozone climatology for UGAMP models.* UK Universities Global Atmospheric Modelling Programme, Internal Report 35.

Lorenz DJ, DeWeaver ET. 2007. Tropopause height and zonal wind response to global warming in the IPCC scenario integrations. *J. Geophys. Res. (Atmos.)* **112**: 10119, DOI: 10.1029/2006JD008087.

McLandress C, Shepherd TG. 2009a. Impact of climate change on stratospheric sudden warmings as simulated by the Canadian Middle Atmosphere Model. *J. Climate* **22**: 5449–5463.

McLandress C, Shepherd TG. 2009b. Simulated anthropogenic changes in the Brewer–Dobson circulation, including its extension to high latitudes. *J. Climate* **22**: 1516–1540.

Pope VD, Gallani ML, Rowntree PR, Stratton RA. 2000. The impact of new physical parametrizations in the Hadley Centre climate model: HadAM3. *Clim. Dyn.* **16**: 123–146.

Ramaswamy V, Chanin M-L, Angell J, Barnett J, Gaffen DJ, Gelman M, Keckhut P, Koshelkov Y, Labitzke K, Lin J-JR, O'Neill A, Nash J, Randel W, Rood R, Shine K, Shiotani M, Swinbank R. 2001. Stratospheric temperature trends: Observations and model simulations. *Rev. Geophys.* **39**: 71–122.

Randel WJ, Shine KP, Austin J, Barnett J, Claud C, Gillett NP, Keckhut P, Langematz U, Lin R, Long C, Mears C, Miller A, Nash J, Seidel DJ, Thompson DWJ, Wu F, Yoden S. 2009. An update of observed stratospheric temperature trends. *J. Geophys. Res. (Atmos.)* **114**: 2007, DOI: 10.1029/2008JD010421.

Rind D, Shindell D, Lonergan P, Balachandran NK. 1998. Climate change and the middle atmosphere. Part III: The doubled CO_2 climate revisited. *J. Climate* **11**: 876–894.

Scaife AA, Knight JR, Vallis GK, Folland CK. 2005. A stratospheric influence on the winter NAO and North Atlantic surface climate. *Geophys. Res. Lett.* **32**: 18715, DOI: 10.1029/2005GL023226.

Schnadt C, Dameris M, Ponater M, Hein R, Grewe V, Steil B. 2002. Interaction of atmospheric chemistry and climate and its impact on stratospheric ozone. *Clim. Dyn.* **18**: 501–517.

Shine KP. 1987. The middle atmosphere in the absence of dynamical heat fluxes. *Q. J. R. Meteorol. Soc.* **113**: 603–633.

Sigmond M, Scinocca JF. 2010. The influence of basic state on the Northern Hemisphere circulation response to climate change. *J. Clim.* **23**: 1434–1446.

